Stimulated parametric polariton-polariton scattering in GaAs microcavities with a shallow polariton band under resonant excitation of exciton mode

A. A. Demenev, S. S. Gavrilov, and V. D. Kulakovskii
Institute of Solid State Physics, RAS, Chernogolovka, 142432, Russia
(Received 21 January 2011; revised manuscript received 29 May 2011; published 19 August 2011)

Energy and spin relaxation of exciton-polaritons and their condensation in momentum (k) space have been investigated in planar GaAs microcavities with a shallow ($\sim$3 meV) low polariton (LP) branch under quasiresonant optical pumping slightly above the exciton energy with ns-long pulses at large k using the time-resolved technique. Nearly 80% depolarization of circularly (σ) polarized photoexcited LPs and the complete depolarization of the linearly (π) polarized LPs are observed during their energy relaxation into the intermediate range of $k \sim 1.5\ \mu\text{m}^{-1}$. In spite of that fact the macro-occupied state formed at $k = 0$ is found to be highly polarized, the degree of its circular polarization under σ-polarized excitation reached 0.9, whereas a linear polarization of the condensate formed under the π-polarized excitation is rotated by 90° with respect to that of the pump. The macrooccupation of the LP state at zero k is reaches at the very beginning of the pulse, but turns out to be unstable, decaying in less than 100 ps. The above features indicate that the population of the condensed mode is mainly provided by stimulated parametric LP-LP scattering directly in the driven mode rather than by quasi-equilibrium Bose-Einstein condensation.

DOI: 10.1103/PhysRevB.84.085305 PACS number(s): 71.36.+c, 42.65.Pc, 42.55.Sa

I. INTRODUCTION

Exciton-polaritons in microcavities (MC) are composite quasi-two-dimensional weakly interacting bosons.[1,2] Despite their short radiative lifetime $\sim 10^{-12}$ s, stimulated scattering toward their ground state has been demonstrated,[3,4] and macrooccupation of the ground state has been recently reported in various MCs under nonresonant excitation.[5–13] As a result, MC polaritons have attracted considerable attention as candidates for Bose-Einstein condensation and are expected to give rise to a Kosterlitz-Thouless phase transition toward superfluidity.[14]

The quasi-two-dimensionality of polaritons, along with their dual exciton-photon character, enables precise optical studies of polariton distribution in momentum (k) space. In GaAs-based MCs with a Q factor of 3000 or less the phonon-assisted energy relaxation is ineffective due to a relatively long scattering time (τ_{ph}) compared to the low polariton (LP) lifetime τ_{LP}: $\tau_{\text{ph}}/\tau_{\text{LP}} \gtrsim 1$ (Refs. 15 and 16). The macrooccupation of states at the LP band bottom is reached at high excitation densities P and initiated mainly by LP-LP scattering, its rate increasing with polariton density n_{LP}.

The lowest threshold excitation density P_{thr} for the realization of the macrooccupied state at the LP band bottom is observed under resonant excitation near the inflection point of the LP branch ($k_p \sim k_{\text{infl}}$) (Refs. 17–21). The macrooccupation is achieved by stimulated parametric LP-LP scattering in the driven mode resulting in the formation of two well-pronounced macrooccupied modes at $k \sim 0$ and $2k_p$. This mechanism is very effective at $k_p \sim k_{\text{infl}}$ due to the simultaneous fulfillment of energy and momentum conservation laws upon scattering of two LPs in the driven mode. The actual stability of the three-mode ($k = 0$, k_p, and $2k_p$) pattern is maintained by the presence of numerous weak "above-condensate" modes, so that the whole system appears to be highly correlated, and the phenomenon is well described within the framework of the model of the dynamically self-organized optical parametric oscillator.[22,23]

Under excitation out of the inflection point of the polariton dispersion, the realization of the condensed $k = 0$ state demands much higher excitation densities[2,6–8,11,13,17] and condensation is reached only in shallow LP bands where the photon contribution in LP states does not exceed 50–60%. The final energy distribution of polaritons in the LP band is usually compared to the quasi-equilibrium Bose-Einstein distribution of spinless particles[5,12,25,26] neglecting the fact that the LP system is inherently dynamical because of short, less than 10 ps, τ_{LP}. In recent studies of an LP condensate formation in CdTe- and GaN-based MCs in a wide range of temperatures there were found that a kinetic condensation regime (when the distribution is not thermal and the threshold is governed by the relaxation kinetics) dominates at low temperatures and negative detuning whereas the thermodynamic regime can be reached at elevated temperatures and positive detunings.[24,27] The consideration was carried without taking into account the LP spin degree of freedom that involves further complications due to the interplay between energy and spin relaxation.[2,28–32]

The LP energy and spin relaxation mechanisms in highly excited LPs in GaAs-based MCs have been recently investigated by Rumpos *et al.*[13] using pulsed pumping at large $k_p \sim 7\ \mu\text{m}^{-1}$ at the exciton resonance wavelength and time integrated registration. In addition to the strong difference in the LP relaxation under excitation with a circularly (σ) and linearly (π) polarized light, the authors revealed an unexpected behavior of LP condensate polarization under π polarized pumping, namely, the LPs condensate demonstrated a linear polarization axis rotated by 90° relative to that of the exciting pump. The suggested explanation assuming that the condensate population by photoexcited LPs occurs upon multiple phonon scattering without loss of their polarization and only one LP-LP scattering act is doubtful since no conservation of linear polarization is usually observed at low excitation densities when the phonon-assisted scattering of LPs is highly dominant.

Here, we report the study of LP condensation in shallow LP bands with $E_X - E_{\rm LP}(k=0) \sim 3$ meV (i. e., in MCs with positive exciton-photon detuning) based on the time resolved polarization-dependent measurements of LP emission under pulsed pumping with long, of about 1 ns, pulses at the exciton resonance wavelength. The use of a high time resolution along with the long duration of exciting pulses allows tracing both spin and k relaxation of LPs and the formation of the LP condensate. The LP condensate polarization found in the experiment—circular in the case of σ excitation and linear inverted relative to that of the exciting pump in the case of π excitation—is similar to that reported by Roumpos *et al.* carried out the measurements only at $k = 0$ (Ref. 13). At the same time, in our additional measurements in a wide range of **k**, no conservation of polarization of photoexcited linearly polarized LPs was revealed after multiple phonon scatterings in the intermediate range of $|\mathbf{k}|$ near the inflection point of the LP dispersion curve at $k = k_{\rm infl} \sim 1.5\ \mu{\rm m}^{-1}$. The LP emission in this range demonstrates a weak linear polarization along the direction of the **k** vector independent of the excitation polarization and density and related to the partial thermalization of LPs between the split transverse electric (TE) and transverse magnetic (TM) modes.

The high linear polarization inverted relative to that of the exciting pump alongside the depolarization of scattered LPs in the intermediate range of k indicates that the population of the condensed mode is due to stimulated parametric LP-LP scattering directly in the driven mode without multiple phonon-scattering events.

In Sec. II we describe our experimental setup. The LP emission properties under excitation with circularly and linearly polarized light are represented in Secs. III and IV, respectively. Section V describes the LP emission kinetics. The LP relaxation mechanisms are discussed in detail in Sec. VI. The conclusions are drawn in Sec. VII.

II. EXPERIMENTAL SETUP

The MC structure was grown by metal organic vapor phase epitaxy. The Bragg reflectors were composed of 17(20) repeats of $\lambda/4$ $Al_{0.13}Ga_{0.87}As/AlAs$ layers in the top (bottom) mirrors. The $3/2\lambda$ GaAs cavity contained six 10-nm thick $In_{0.06}Ga_{0.94}As/GaAs$ quantum wells (QWs). The Rabi splitting was 6 meV. A gradual variation of the active layer thickness along the sample involves a change in photon mode energy E_C and, accordingly, in detuning δ between exciton $E_X(k=0)$ and photon $E_C(k=0)$ mode energies. The experiments were carried out on several spots with $\delta = E_C - E_X \sim 1$ meV.

The sample was placed into an optical cryostat with controlled temperature. A pulsed Ti-sapphire laser with a pulse duration of ~1.5 ps, line full width at half maximum (FWHM) of ~1 meV, and pulse repetition of 5 kHz was used for excitation of the MC at the angle 40° ($k_p = 4.8\ \mu{\rm m}^{-1}$) relative to the cavity normal. The pump beam was focused onto a spot 100 μm in diameter after passing through a long multimode fiber resulting in the increasing of the pulse duration to ~1.5 ns. The kinetics of the angular distribution of the LP emission signal from the MC was detected in a wide solid angle (30°) around the cavity normal by a streak camera with spectral, angular, and time resolution of 0.28 meV, 0.05 $\mu{\rm m}^{-1}$, and 70 ps, respectively.

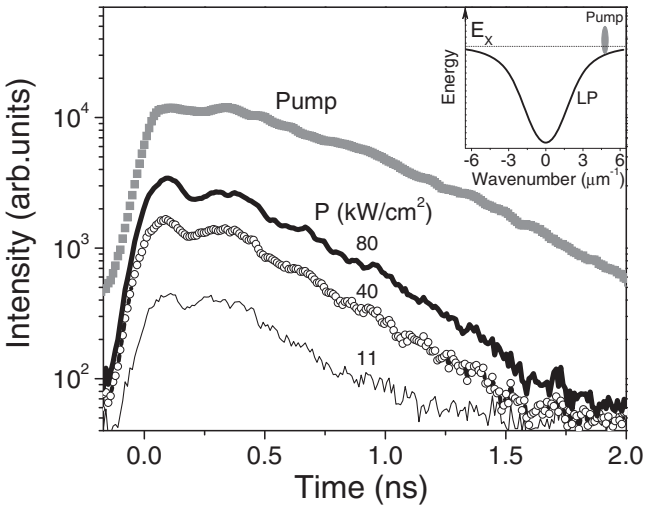

FIG. 1. Time dependences of pump and transmission intensity recorded at $k = k_p$ and various excitation densities P. Inset shows schematical LP and exciton dispersion curves.

III. LP EMISSION UNDER EXCITATION WITH CIRCULARLY POLARIZED LIGHT

A pump pulse profile $I_p(t)$ proportional to the intensity of the external electric field outside the MC $|E_{\rm ext}(k_p,t)|^2$ is shown in Fig. 1. The intensity builds up during the first 100 ps, remains nearly constant during approximately 300 ps, and then decreases slowly (by a factor of 3 to $t = 1$ ns). Circularly or linearly polarized pulses excite the MC at ~0.3 meV above E_X at $k_p = (k_{px},k_{py}) = (4.8,0)\ \mu{\rm m}^{-1}$ as shown in the inset in Fig. 1. Figure 1 shows the recorded kinetics of the MC transmission signal, $I_{tr}(t)$, that is proportional to the electric field at the QW, $|E_{\rm QW}(k_p,t)|^2$, at various excitation densities. It is seen that the ratio $|E_{\rm QW}(k_p,t)|^2/|E_{\rm ext}(k_p,t)|^2$ decreases rather weakly with time both at low and high excitation densities, and no marked instabilities and/or hysteresis effects the characteristic of excitation near the inflection point of the LP dispersion curve are observed.[33]

Figures 2(d)–2(f) show the k distribution of LP emission in the MC with $\delta = +1$ meV recorded in the range of $|\mathbf{k}| < 2\ \mu{\rm m}^{-1}$ in the time-integrated mode for $P =$ 5, 20, and 80 kW/cm^2, respectively, with σ^+-polarized light. It is seen that the distribution of LP emission is nearly axially symmetric in k space with maximum intensity $I_{\rm LP}(\mathbf{k})$ at $k = 0$. No pronounced bottleneck is observed even at the lowest excitation density. The behavior of LP emission spectra at various P is illustrated in Figs. 2(a)–2(c) displaying the dependences $I_{\rm LP}(E,k_y)$ at $k_x = 0$. It is seen that the spectra demonstrate a well-pronounced blue shift of the LP transition energies $E_{\rm LP}(k)$ with increasing P. The shift is connected to an enhanced LP-LP interaction. A comparison of Figs. 2(a) – 2(f) shows a well-pronounced gradual shrinkage of the LP emission in both the energy scale and k space with increasing P.

The dependences of $I_{\rm LP}(k=0)$, $E_{\rm LP}(k=0)$, and the full width of the LP emission intensity at half maximum (FWHM)

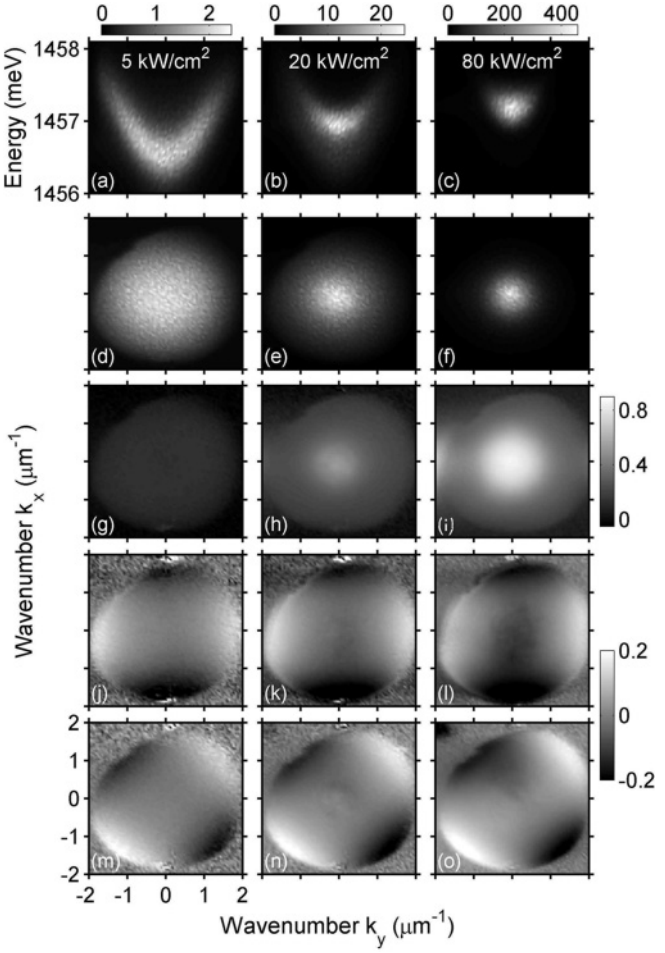

FIG. 2. (a–c) k_y dependence of LP emission spectra at $k_x = 0$, (d–f) **k** distributions of LP emission intensity, and (g–i) polarization degrees ρ_{circ}, (j–l) $\rho_{\mathrm{lin},y}$, and (m–o) $\rho_{\mathrm{lin},y'}$ in the MC with $\delta = +1$ meV recorded in the range of $|\mathbf{k}| < 2\ \mu\mathrm{m}^{-1}$ in the time integrated mode under excitation with σ^+-polarized light and various excitation densities $P = 5$ kW/cm^2 (left panel), 20 kW/cm^2 (middle panel), and 80 kW/cm^2 (right panel), respectively.

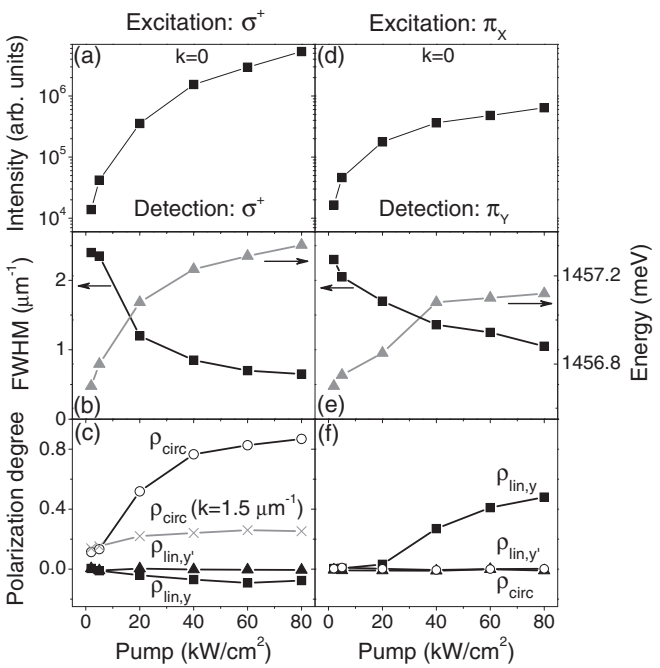

FIG. 3. The dependences of (a, d) LP emission intensity $I_{\mathrm{LP}}(k = 0)$, (b, e) transition energy $E_{\mathrm{LP}}(k = 0)$ and FWHM of the LP emission in $k-$space, Δk_{FWHM}, and (c, f) LP polarization degrees $\rho_{\mathrm{circ}}(k = 0)$, $\rho_{\mathrm{lin},y}(k = 0)$, and $\rho_{\mathrm{lin},y'}(k = 0)$ on P under excitation with circularly (left panel) and linearly (right panel) polarized pulses. Figure (c) shows as well $\rho_{\mathrm{circ}}(k = 1.5\ \mu\mathrm{m}^{-1})$.

in k space, Δk_{FWHM}, on P are displayed in Fig. 3. Figure 3(a) shows that the increase in P from 2 to 80 kW/cm^2 results in the increase in $I_{\mathrm{LP}}(0)$ exceeding two orders of magnitude. This increase is followed by a decrease in Δk_{FWHM} from $\sim$2.4 to $\sim$0.6 $\mu\mathrm{m}^{-1}$ and a blue shift in $E_{\mathrm{LP}}(k = 0)$ reaching $\sim$0.65 $\pm$ 0.03 meV as shown in Fig. 3(b) .

A threshold increase of LP emission intensity $I_{\mathrm{LP}}(k = 0)$ with a simultaneous sharp narrowing of the LP emission in k space can occur due to either a direct stimulated parametric scattering of LPs in the driven mode or an LP condensation in the photoexcited LP system via multiple LP scattering. In the first case the phenomenon can be described within the framework of the model of the optical parametric oscillator (OPO) similar to the one used in the case of excitation near k_{infl} (Refs. 34–37) whereas in the latter case it is described in terms of quasithermal LP condensation in k space.[2,5,24–27,38]

Additional information on the dominating mechanism of LP relaxation toward the band bottom has been obtained from polarization measurements. The polarization properties of LP emission under excitation with σ^+-polarized pulses are illustrated in Figs. 2(g) –2(o) . The degrees of circular polarization $[\rho_{\mathrm{circ}}(k) = (I^+_{\mathrm{LP}}(k) - I^-_{\mathrm{LP}}(k)]/[I^+_{\mathrm{LP}}(k) + I^-_{\mathrm{LP}}(k)]$ are presented in Figs. 2(g) – 2(i)–2(j), –2(l), and 2(m)–2(o) and show the degrees of linear polarizations $\rho_{\mathrm{lin},y}(k) = [I^y_{\mathrm{LP}}(k) - I^x_{\mathrm{LP}}(k)]/[I^y_{\mathrm{LP}}(k) + I^x_{\mathrm{LP}}(k)]$ and $\rho_{\mathrm{lin},y'}(k) = [I^{y'}_{\mathrm{LP}}(k) - I^{x'}_{\mathrm{LP}}(k)]/[I^{y'}_{\mathrm{LP}}(k) + I^{x'}_{\mathrm{LP}}(k)]$, respectively. Here I^i_{LP} are the LP emission intensities recorded in σ^+, σ^-, π_x, π_y, π_{x+y}, and π_{x-y} polarizations for $i = \sigma^+$, σ^-, x, y, x', and y', respectively.

The LPs excited by σ^+-polarized pulses with $P = 5$ kW/cm^2 gradually lose their circular polarization during relaxation to the LP band bottom. That is illustrated in more detail in Fig. 4 displaying the dependence of $\rho_{\mathrm{circ}}(k_x)$ at $k_y = 0$. It shows that $\rho_{\mathrm{circ}}(k \sim 1.5\ \mu\mathrm{m}^{-1}) \sim 0.16$ at $P = 5$ kW/cm^2 and decreases gradually to ~ 0.13 at $k = 0$. A monotonous decrease in ρ_{circ} approaching the band bottom is connected with LP depolarization in the process of multiple phonon assisted LP scattering processes providing their energy relaxation.

Figures 2(j)– 2(o) show that, simultaneously with the loss of circular polarization, the LPs gain a linear polarization in the range of $|\mathbf{k}| = 1$–$2\ \mu\mathrm{m}^{-1}$ and lose it when approaching the LP band bottom. The magnitude of $\rho_{\mathrm{lin},y}(\mathbf{k})$ at $|\mathbf{k}| \sim 1.5\ \mu\mathrm{m}^{-1}$ is maximum at $\mathbf{k} \| 0y$, vanishes at $\mathbf{k} \| 0y'$ and $0x'$, and reaches a maximum negative value at $\mathbf{k} \| 0x$. By contrast, the magnitude of $\rho_{\mathrm{lin},y'}(|\mathbf{k}| \sim 1.5\ \mu\mathrm{m}^{-1})$ is maximum at $\mathbf{k} \| 0y'$, vanishes at $\mathbf{k} \| 0y$ and $0x$, and reaches a maximum negative value at $\mathbf{k} \| 0x'$. Such behavior of the linear polarization of LP emission indicates that the linear polarization of LPs is directed along the LP **k** vector.

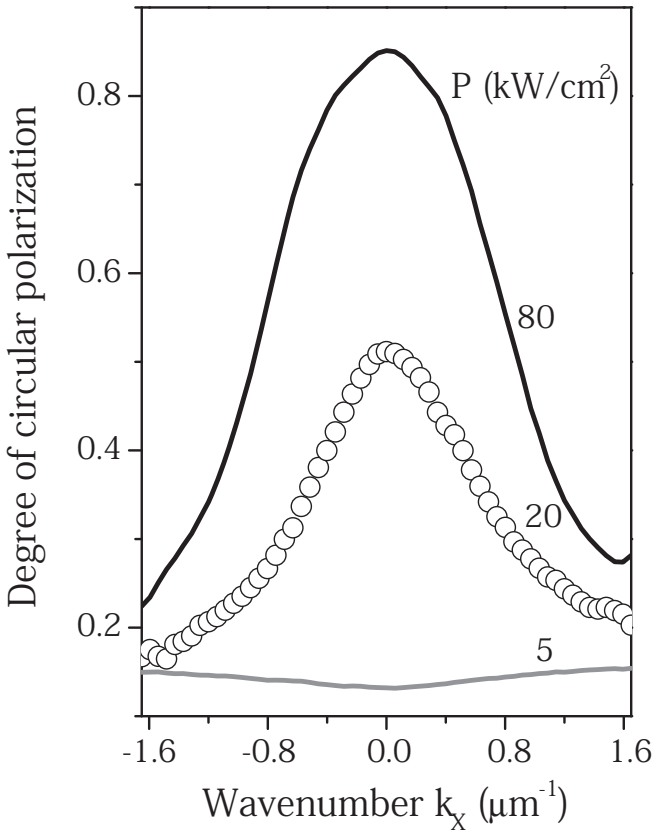

FIG. 4. Dependences $\rho_{\rm circ}(k_x)$ at $k_y = 0$ in the MC with $\delta = +1$ meV recorded in the integrated mode under excitation with σ^+-polarized light and various excitation densities $P = 5$, 20, and 80 kW/cm^2.

The small linear polarization of LP emission is natural to connect with a partial thermalization of LPs between the two split (TE and TM) LP modes. In the case of LPs under thermal equilibrium, $|\rho_{\rm lin}| \approx \Delta/2k_{\rm B}T$ for the TE/TM splitting Δ being less than $k_{\rm B}T$. The magnitude of $|\rho_{\rm lin}|$ at $k \approx 0.18\,\mu$m^{-1} is equal to 0.12 ± 0.03, and decreases down to 0.02 ± 0.03 at $k = 0$; $T_{\rm bath} \approx 6$ K in a wide range of $P < 40$ kW/cm^2. Thereby one can estimate Δ to be increasing from 0 to 0.12 meV with the increase in k from 0 to 1.8 μm^{-1}. Note that $|\rho_{\rm lin}(k)|$ exhibits nearly axial symmetry, and nearly vanishes at $k \to 0$. Thereby a relatively large value of TE-TM splitting at $k \sim 1.5$ μm^{-1} seems to be caused by a dislocation of the cavity mode with respect to the center of the Bragg mirror refraction band rather than by the lowered MC symmetry.

Figures 2(h) and 2(i) show that the decrease in $\rho_{\rm circ}$ of LPs at $\mathbf{k} \to 0$ changes with increasing P into the strong increase. The latter is shown in detail in Fig. 4 displaying the dependences $\rho_{\rm circ}(k_x)$ at $k_y = 0$ for various P. It is seen that $\rho_{\rm circ}(k_x)$ at 5 kW/cm^2 decreases gradually from 0.16 to 0.13 when k_x decreases from 1.6 μm^{-1} to 0. At $P = 20$ kW/cm^2, $\rho_{\rm circ}(k_x = 1.6\ \mu$m$^{-1}) \sim 0.2$, changes weakly in the range of $k_x = 1$–1.6 μm^{-1} and then increases up to 0.5 at $k_x = 0$. An increase in P to 80 kW/cm^2 results in a rather weak increase in $\rho_{\rm circ}$ in the range of $k_x = 1$–1.6 μm^{-1} whereas $\rho_{\rm circ}$ at smaller k_x increases strongly resulting in $\rho_{\rm circ}(k = 0) \sim 0.87$.

A comparison of the dependences $\rho_{\rm circ}(P)$ and $I_{\rm LP}(P)$ at $k = 0$ in Figs. 3(a) and3(c) shows that the strong increase in $\rho_{\rm circ}(k = 0)$ starts at $P = 5$ kW/cm^2, which is only slightly delayed with respect to the threshold increase in $I_{\rm LP}(k = 0)$. That allows one to suppose that the strong increase in $\rho_{\rm circ}(k = 0)$ at large P is caused by an effect of the stimulated scattering of LPs into the $k = 0$ state when its occupation factor exceeds the critical one.

In general, the weakening of depolarization of σ^+-polarized LPs during their energy relaxation is well expected at high P because of an increased contribution of LP-LP scattering to the LP relaxation process. That is related to the fact that the LP-LP scattering occurs with the conservation of circular polarization due to the angular momentum conservation law. However, the sharp growth of $\rho_{\rm circ}(k)$ observed at small k in highly excited MCs demands a further discussion.

IV. LP EMISSION UNDER EXCITATION WITH LINEARLY POLARIZED LIGHT

Additional information on the mechanism of LP relaxation to the band bottom is provided by polarization measurements of LP emission under linearly polarized pulses. The scattering of two collinearly polarized LPs results in the rotation of their linear polarization by 90 degrees,[39–41] which allows to trace LP-LP scattering acts of photoexcited LPs. Figures 5(d)–5(f) show the **k** distribution of LP emission intensity excited with

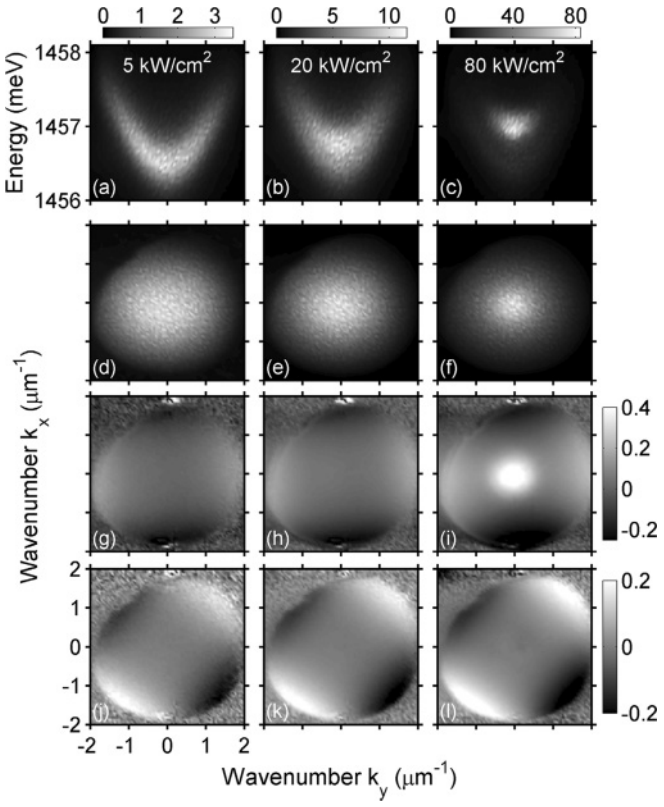

FIG. 5. (a–c) k_y dependence of LP emission spectra at $k_x = 0$, (d–f) k distribution of LP emission intensity, and (g–i) degrees of linear $\rho_{{\rm lin},y}$ and (j–l) $\rho_{{\rm lin},y'}$ polarization in the MC with $\delta = +1$ meV recorded in the range of $|\mathbf{k}| < 2$ μm^{-1} in the time integrated mode under excitation with π_x-polarized light and various excitation densities $P = 5$ kW/cm^2 (left panel), 20 kW/cm^2 (middle panel), and 80 kW/cm^2 (right panel), respectively.

linearly (π_x) polarized pulses and recorded in π_y polarization in the time integrated mode, whereas Figs. 5(a) – 5(c) display the LP emission spectra at $k_x = 0$ as functions of energy and k_y for the same excitation densities.

The behavior of both the energy and **k** distribution of LP emission intensity under excitation with π_x-polarized light is qualitatively similar to the behavior under excitation with σ^+-polarized pulses shown in Fig. 2. The angular distribution of $I_{\rm LP}$ is almost independent of the direction of the **k** vector and does not reveal any marked bottleneck already at the lowest excitation density. The increase in P leads to a superlinear increase of the LP emission intensity, its blue shift and shrinkage in k space. They are, however, somewhat smaller than under σ^+-polarized excitation. This is well seen from the comparison of Figs. 3(a) –3(c) and3(d) –3(f) that show the experimental dependences $I_{\rm LP}(P)$, $\Delta k_{\rm FWHM}(P)$, and $\Delta E(P)$ at $k = 0$ for the cases of excitation with σ^+- and π_x-polarized pulses, respectively.

No circular polarization of the LP emission has been observed under excitation with π_x-polarized pulses. The linear polarization of the LP emission is shown in Figs. 5(g) – 5(l). A comparison of Figs. 5(g) and 5(j) with Figs.2(j) and 2(m) show that the linear polarization of LP emission at $P = 5$ kW/cm^2 is very similar to that observed under excitation with σ^+-polarized pulses. The dominant polarization direction at $|\mathbf{k}| \sim 1.5\ \mu$m^{-1} coincides with that of the LP **k** vector: $\rho_{{\rm lin},y}$ ($\rho_{{\rm lin},y'}$) is maximum at $\mathbf{k}\|0y$ ($\mathbf{k}\|0y'$), vanishes at $\mathbf{k}\|0y'$ and $0x'$ ($\mathbf{k}\|0y$ and $0x$), and reaches a maximum negative value at $\mathbf{k}\|0x$ ($\mathbf{k}\|0x'$), the maximum degree of linear polarization does not exceed 0.2. No linear polarization is observed at $k = 0$.

Figures 5(g) and 5(h) and 5(j) and 5(k) show that the linear polarization of LPs at $|\mathbf{k}| \sim 1.5\ \mu$m^{-1} depends very weakly on the excitation power. On the other hand, the emission at $k = 0$ remains unpolarized only at $P \lesssim 20$ kW/cm^2, whereas $\rho_{{\rm lin},y}$ at $P = 80$ kW/cm^2 appears to be as high as ~0.5. Figure 3 shows that the sharp increase in $\rho_{{\rm lin},y}$ under excitation with linearly polarized pulses starts at $P > 20$ kW/cm^2 (i.e., it occurs at markedly higher P than the sharp increase in the emission intensity). The polarization is directed along $0y$ (i.e., along a normal to the direction of polarization of excitation pulses). Such behavior of the linear polarization of LPs at $k = 0$ indicates that this state is populated mainly via scattering of LPs with π_x polarization. This observation is similar to that in Ref. 13.

V. KINETICS OF LP EMISSION INTENSITY AND POLARIZATION

Time dependences of the LP emission intensity in the range of $k_x \lesssim 2\ \mu$m^{-1} measured with time resolution of 70 ps at various excitation densities are represented in Figs. 6(a)–6(d) and 7(a)–7(e) for σ^+- and π_x-polarized excitations, respectively. A comparison of these figures shows that the time dependences of $I_{\rm LP}(k)$ under σ^+- and π_x-polarized excitations are similar to each other. In particular, Figs. 6(a) and 7(a) show that in both cases the maximum emission $I_{\rm LP}(k = 0)$ at $P = 5$ kW/cm^2 is markedly, by ~0.3 ns, delayed with respect to the maximum in $I_p(t)$. The delay is of the order of the lifetime of excitons in the InGaAs QWs and seems to be connected with an accumulation of exciton-like LPs

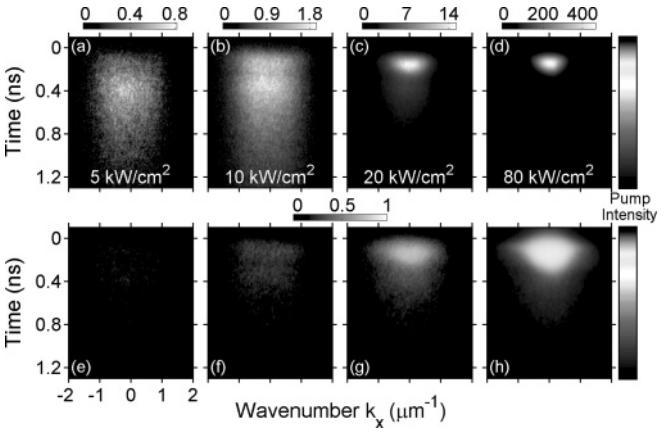

FIG. 6. Time dependences of LP emission intensity (upper array) and degree of circular polarization (lower array) in the range of $k_x \lesssim 2\ \mu$m^{-1} at $k_y = 0$ measured under the excitation with circularly polarized pulses at various excitation densities (a, e) $P = 5$, (b, f) 10, (c, g) 20, and (d, h) 80 kW/cm^2. Excitation pulse profile is shown in the right column in the upper and lower arrays.

in states with large k. The increase in the LP-LP scattering rate in a dense LP system with increasing P leads to the disappearance of this delay. Figures 6(b) and 7(b) show that the delay disappears already at $P = 10$ kW/cm^2.

At larger excitation densities (Figs. 6(c) and 6(d) and 7(c)–7(e)) $I_{\rm LP}(k)$, by contrast, demonstrates a sharp growth in the whole range of k at the very beginning of the exciting pulse, which changes abruptly to an even sharper decrease well before the decrease in the excitation density $I_p(t)$. That is better seen in Figs. 8(a) –8(d) displaying time dependences of $I_{\rm LP}(t)$ at $k = 0$ and $k = k_{\rm infl} = 1.5\ \mu$m^{-1} at various P in more detail. It is clearly seen that the dependence $I_{\rm LP}(k = 0,t)$ nearly coincides with $I_p(t)$ under the excitation with σ- and π-polarized pulses only at $P = 10$ kW/cm^2. At higher P, the duration of a strong signal at both $k = 0$ and $k \sim k_{\rm infl}$ is about 0.25 ns in the case of excitation with σ^+-polarized pulses and does not exceed 0.2 ns in the case of π_x-polarized pulses in spite of the fact

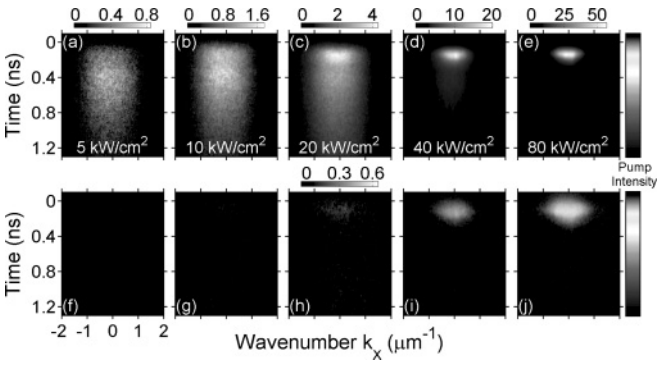

FIG. 7. Time dependences of LP emission intensity (upper array) and degree of linear $\rho_{{\rm lin},y}$ polarization (lower array) in the range of $k_x \lesssim 2\ \mu$m^{-1} at $k_y = 0$ measured under the excitation with π_x polarized pulses at various excitation densities (a, f) $P = 5$, (b, g) 10, (c, h) 20, (d, i) 40, and (e, j) 80 kW/cm^2. Excitation pulse profile is shown in the right column in the upper and lower arrays.

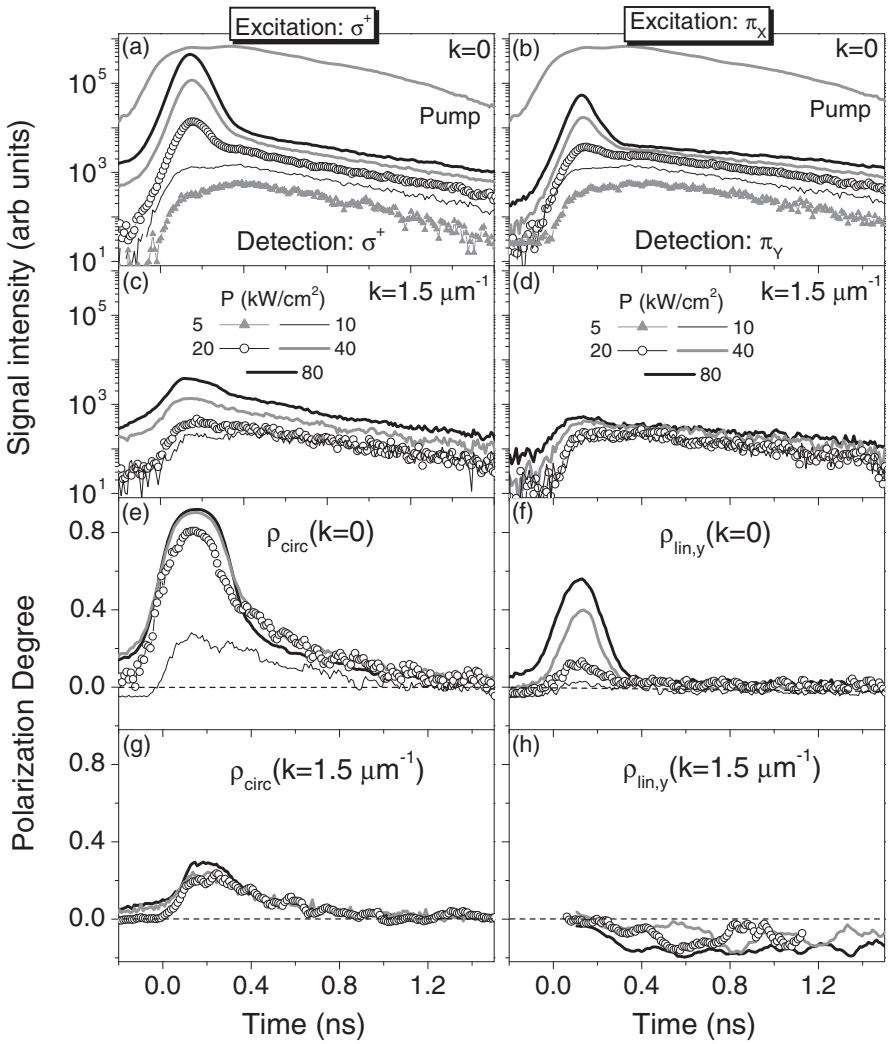

FIG. 8. Time dependences of LP emission intensity and polarization degree under the excitation with σ^+ (left panel) and π_x (right panel) polarized pulses. $I_{\rm LP}$ at $k = 0$ and 1.5 μm^{-1} are shown in (a,b) and (c,d), respectively. $\rho_{\rm circ}$ at $k = 0$ and 1.5 μm^{-1} are shown in (e) and (g), respectively. $\rho_{{\rm lin},y}$ at $k = 0$ and 1.5 μm^{-1} are shown in (f) and (h), respectively. Pump pulse profile is shown by thick gray line in (a,b).

that I_p starts to decrease only in 0.3 ns [i.e., no quasistationary regime of LP emission is established in the range of nearly constant $I_p(t)$ in both cases].

A comparison of time dependences $I_{\rm LP}(k,t)$ at $k = 0$ and $k = 1.5\mu$m^{-1} in Figs. 6–8 shows that at both σ^+ and π_x-polarized excitations there is no direct connection between the population of the states in the range of $k \sim k_{\rm infl}$ and the threshold increase in the population of the $k = 0$ state. Indeed, it is seen that at all $P > 10$ kW/cm^2 the population of states at $k \sim k_{\rm infl}$ is orders of magnitude smaller than that at $k = 0$. Further, Fig. 8 shows that the sharp growth of the signal at $k = 0$ is well pronounced already at $P = 20$ kW/cm^2 whereas that in the range of $k = 1.5$ μm^{-1} occurs only at $P = 40$ kW/cm^2, at both σ^+ and π_x-polarized excitations.

The time dependences of $\rho_{\rm circ}(k_x,t)$ at $k_y = 0$ for excitations with σ^+-polarized pulses are shown in Figs. 6(e)–6(h). It is seen that the pronounced time dependence in $\rho_{\rm circ}(k_x,t)$ appears only at $P = 10$ kW/cm^2 when $\rho_{\rm circ}(t)$ at all k_x increases and then decreases following the time dependence of the LP emission intensity. As was mentioned above, such dependence is well explained by an enhanced contribution of LP-LP scattering in the energy relaxation of photoexcited circularly polarized LPs. An increase in P above 20 kW/cm^2 results in a sharp increase in $\rho_{\rm circ}(k = 0)$ up to the values of 0.8–0.9. The increase coincides with a threshold growth of $k = 0$ population. A comparison of Figs. 8(a) and 8(e) shows as well that the strong circular polarization of LPs at $k = 0$ disappears simultaneously with the decrease in the density of LPs at $k = 0$ rather than with the decrease in $I_p(t)$.

Figure 8(g) shows that the LP polarization at large k is much smaller than at that $k = 0$. The value of $\rho_{\rm circ}$ at $k \sim 1.5$ μm^{-1} depends very weakly on time and the excitation density and does not exceed 0.3.

The time dependences of $\rho_{{\rm lin},y}(k_x,t)$ at $k_y = 0$ for the excitations with π_x-polarized pulses are shown in Figs. 7(f)–7(j). $\rho_{{\rm lin},y}(k_x,t)$ at $P \leqslant 20$ kW/cm^2 is very small in the whole range of k_x and t. A pronounced short-duration increase in $\rho_{{\rm lin},y}(k_x,t)$ is observed only at $P \gtrsim 40$ kW/cm^2 and occurs only at $k \sim 0$. It coincides in time with a short-duration increase in $I_{\rm LP}(k = 0)$. A comparison of dependences $\rho_{{\rm lin},y}(t)$ and $\rho_{\rm circ}(t)$ at $k = 0$ in Fig. 8 shows that they are qualitatively very similar, however, the maximum values of $\rho_{\rm lin}(k = 0)$ are markedly smaller. In particular, $\rho_{\rm circ}(k = 0)$ at $P = 80$ kW/cm^2 reaches 0.9 whereas $\rho_{\rm lin}(k = 0)$ does not exceed 0.6. Note that the smaller value of $\rho_{\rm lin}(k = 0)$ correlates with a markedly smaller

LP population at $k = 0$ in MCs excited with π_x-polarized light as it is seen from a comparison of the LP emission intensities in Figs. 8(a) and 8(b). Finally, Fig. 8(h) shows that $|\rho_{\mathrm{lin},y}|$ at $k \sim 1.5\ \mu\mathrm{m}^{-1}$ remains small (<0.2) in the whole range of excitation densities and does not change its orientation along the LP **k** vector during the excitation pulse.

Thus, the experiment shows no correlations between the population and polarization of LPs at $k = 0$ and those at $k \sim k_{\mathrm{infl}}$, which indicates that the threshold macropopulation of the $k = 0$ state cannot be due to the stimulated scattering of LPs from $k \sim k_{\mathrm{infl}}$ as it was proposed in Ref. 13.

VI. LP RELAXATION MECHANISMS

The energy relaxation of LPs in MCs weakly excited at large k at the exciton resonance is mainly achieved by the acoustic phonon assisted LP scattering. In 10-nm thick QWs it can effectively lower the LP energy up to ~1 meV in a single scattering act,[42,43] whereas the bottom of the LP band is located at ~4 meV below $\hbar\omega_{\mathrm{pump}}$. The energy relaxation of photoexcited LPs is realized via multiple scattering of LPs. The latter results as well in the population of long-lived exciton-like LPs with large k, which explains the pronounced delay of maximum $I_{\mathrm{LP}}(k = 0)$ with respect to that of $I_p(t)$. Figures 8(a) and 8(b) show that this delay reaches 0.3 ns at $P \leqslant 5\ \mathrm{kW/cm^2}$, which is just of the order of the average lifetime of long lived LPs with $k \sim 10^6\ \mathrm{cm}^{-1}$. Note as well that a weak dependence of I_{LP} on k at $E < E_X$ at this excitation density indicates that the k distribution of short-lived LPs near the LP band bottom is far from being thermalized.

Multiple phonon-assisted scattering of photoexcited LPs results in their gradual depolarization on approaching the LP band bottom, which is observed in Figs. 2(g) and 4. The growth of average ρ_{circ} at higher P observed in Figs. 2(h)–2(i) , and 4 is well explained, as it was indicated in Sec. III, by an enhanced contribution of LP-LP scattering brought about by the conservation of circular LP polarization in accordance with the momentum conservation law. This scattering also leads to the acceleration of LP energy relaxation resulting in the disappearance of the delay of the maximum in $I_{\mathrm{LP}}(t)$ at $k = 0$ as compared to that in $I_p(t)$ (Figs. 6(a) and 8(a)). At the same time, the increase in $\rho_{\mathrm{circ}}(k)$ at $k \to 0$ observed in Figs 2 and 4 with increasing P demands a more detailed consideration. It is seen in Figs. 6 and 8 that the increase in $\rho_{\mathrm{circ}}(k)$ at $k \to 0$ appears concurrently with the onset of macrooccupation of the $k = 0$ state and disappears nearly simultaneously with its emptying. Figure 6 shows that the higher the density of LPs at $k = 0$ the larger $\rho_{\mathrm{circ}}(k = 0)$.

Thus the magnitude of ρ_{circ} at $k = 0$ correlates with the LP density in this state. Note, however, that circular polarization is not inherent in the thermodynamically equilibrium LP condensate state. This state has to be linearly polarized due to the weaker repulsion interaction between LPs with opposite circular polarizations compared to that between LPs with the same circular polarization. It is seen from a comparison of Figs. 6(g) and 6(h) and 6(c) and 6(d) that the LP system at large k ($>1\ \mu\mathrm{m}^{-1}$) remains weakly polarized in the whole range of times when the $k = 0$ state is macropopulated. Hence, the nearly 100% circular polarization of the LP condensate in such a system indicates that the LP spin state of macropopulated

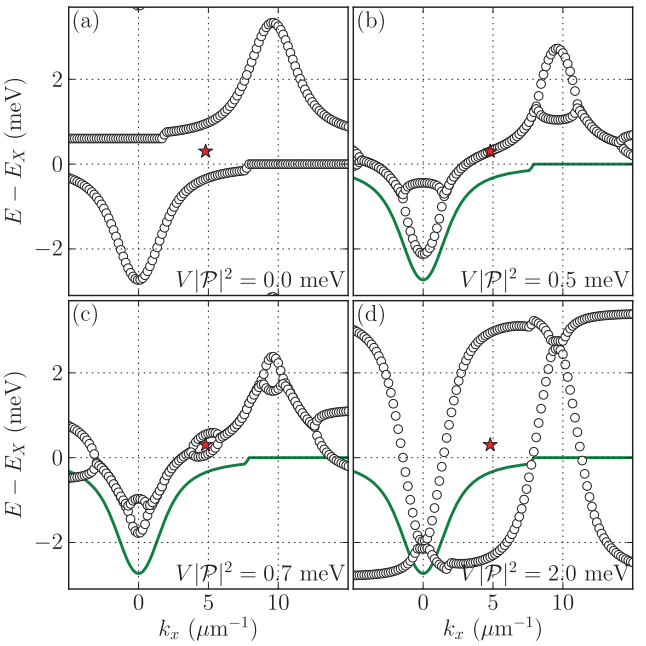

FIG. 9. (Color online) The renormalized dispersion $E(k_x)$ of "signal" and "idler" LP modes in the dependence on the intensity of excitonic component of the driven mode ($V|\mathcal{P}|^2$), calculated in scalar (spinless) approximation. The position of the driven mode is shown by a star and the unperturbed LP dispersion is shown by a solid line.

$k = 0$ state is strongly nonequilibrium. That prevents the interpretation of the observed phenomenon in terms of quasi-equilibrium Bose-Einstein condensation.

The increase in $\rho_{\mathrm{circ}}(k)$ at small k is natural to relate to the stimulated scattering into the macropopulated $k = 0$ mode of LPs from a wide range of $k > 0$. This mechanism activating when the occupation of the low k states exceeds 1 because the bosonic nature of LPs is more effective for the polarization dominating in macropopulated $k = 0$ state. On the other hand, the formation of a high circular polarization of the signal at $k = 0$ can occur due to direct stimulated parametric LP-LP scattering from the driven mode. Being very effective under excitation near k_{infl}, such scattering loses its efficiency with increasing k_p due to the problem with the simultaneous fulfillment of the energy and momentum conservation laws.[17]

To estimate the blue shift necessary to restore the efficiency of the direct LP-LP scattering into the $k = 0$ "signal" in the studied structure, we employ the coherent OPO model.[22] Figure 9 displays the renormalized dispersion of "signal" and "idler" modes in the dependence on $V|\mathcal{P}|^2$, where $\mathcal{P}$ is the amplitude of excitonic field and V is the exciton-exciton interaction constant. The calculations are performed in scalar (spinless) approximation using the Gross-Pitaevskii equations linearized over signal and idler amplitudes, assuming the driven mode amplitude $\mathcal{P}$ to be the governing parameter (see Refs. 22,45, and 46). The cavity dispersion is calculated using the transfer matrix technique.[47] The discontinuity in the unperturbed polariton energy at $k_{\mathrm{wg}} = 7.8\ \mu\mathrm{m}^{-1}$ (solid line) is due to reaching the nondissipative waveguide cavity mode, so that the strong exciton-photon coupling vanishes at $|k| > k_{\mathrm{wg}}$.

The "bare" blue shift of the signal mode, which only depends on the exciton population, is $2V|\mathcal{P}|^2$; it is given by the diagonal elements of the matrix of effective energy of excitations. Besides that, the signal and idler are coupled through the phase-sensitive off-diagonal elements, and the energy matrix as a whole is anti-Hermitian. Due to this coupling, the signal and idler dispersion curves appear to be stuck together in the ranges of maximum effective lifetimes (given by the imaginary parts of eigenenergies) which indicate the predominant directions of parametric scattering.

Figure 9 a shows the unperturbed dispersions ($V|\mathcal{P}|^2 = 0$). In Fig. 9(b) ($V|\mathcal{P}|^2 = 0.5$ meV), the signal and idler dispersions are stuck together the vicinity of the driven mode. This situation is unobservable, as the driven mode by itself is in the unstable area (in between the two branches of stability). The stable solution for the driven mode appears at $V|\mathcal{P}|^2 \gtrsim 0.75$ meV (Fig. 9(c)), after which the dominant directions of scattering shrink into $k = 0$ with the further increase of $|\mathcal{P}|$. Lastly, although the blue shift at $k = k_{\text{pump}}$ exceeds 3 meV at $V|\mathcal{P}|^2 = 2$ meV (Fig. 9(d)), the blue shift of the "signal" polariton mode at $k = 0$ is only about 0.7 meV, in agreement with the experimental observations.

Thus, both the direct LP-LP scattering in the driven mode and the scattering of partially relaxed LPs with $\mathbf{k} \neq \mathbf{k}_p$ in MCs excited with σ^+-polarized pulses contribute to the condensate mode. A separation of these contributions is hardly possible because of their additive character. The situation changes, however, in the MCs excited with linearly polarized light since the direct LP-LP scattering of linearly polarized LPs causes the rotation of their linear polarization.

It is found in Secs. IV and V that the linear polarization of photoexcited LPs gets lost during their energy relaxation in MCs excited with π_x-polarized pulses up to $P \sim 20$ kW/cm^2. The small linear polarization of LP emission observed at $|\mathbf{k}| \sim 1.5\ \mu\text{m}^{-1} \sim k_{\text{infl}}$ is related to the partial thermalization of LPs between the two split (TE and TM) LP modes. Indeed, it follows from Figs. 5(g)–5(j), and 5(k) that it is always directed along the $\mathbf{k}$ vector, whereas the comparison of Figs. 2 and 5 shows that the magnitude of $|\rho_{\text{lin}}|$ does not depend on the direction of the $\mathbf{k}$ vector and even the polarization of the exciting pulses. It is also seen in Figs. 5(i) and 5(l) that the increase in excitation density does not lead to the appearance of any pump-driven linear polarization of LP states at $k \sim k_{\text{infl}}$. Thus, the experiment shows that no conservation of linear polarization of LPs (which was postulated in Ref. 13) occurs upon multiple phonon-assisted and/or LP-LP scattering both at low and high excitation densities. Thus the linear polarization of LP condensate at $k = 0$ cannot be explained by the effect of pairwise LP-LP scattering of LPs relaxed down to $|\mathbf{k}| \sim k_{\text{infl}}$.

The strong linear polarization of the LP condensate excited with linearly polarized pulses can be related either to the spontaneous linear polarization expected in thermodynamically equilibrium LP condensate[11,44] or to the LP-LP scattering in the driven mode.[39–41] The first cause has to be rejected. First, the above discussed experiments with circularly polarized excitation exhibit almost completely circular polarization of the condensate, thereby no thermodynamic equilibrium is reached in the condensate because of a very short, of several ps, LP lifetime. Second, it is worthwhile to note that no fixed linear polarization in symmetric MCs can be registered even in the emission of equilibrium linearly polarized LP condensate in our measurements using averaging over thousands of pulses owing to a random direction of the condensate polarization in each pulse. A fixed direction of polarization in the LP condensate can be realized only in MCs with a lowered symmetry. However, in this case the polarization direction should be pinned to the symmetry axes whereas in our experiments it is linked to the direction of the linear polarization in the driven LP mode. Note as well that the LP condensate at $k = 0$ excited by pulses linearly polarized along the $0x$ direction is polarized along the $0y$ one, whereas the condensate excited by circularly polarized pulses demonstrates a weak preferential linear polarization along the $0x$ direction.

Summarizing the above discussion, one has to conclude that the main contribution to the population of the condensed mode at $k = 0$ originates from the direct stimulated LP-LP scattering in the driven mode and has to be described in the framework of the optical parametric oscillator rather than quasi-equilibrium Bose-Einstein condensation. An additional support to this conclusion comes from the observation discussed in Sec. V of the instability of LP condensate emission in the range of nearly constant $I_p(t)$ under excitation with both σ^+ and π_x-polarized pulses: the sharp increase in the condensate density changes immediately, well before the decrease in $I_p(t)$, into a similar sharp decrease. Such an instability of the condensate mode is more characteristic of a nonlinear LP-LP scattering rather than Bose-Einstein condensate under quasistationary excitation conditions.

VII. CONCLUSION

Exciton-polariton energy and spin relaxation has been investigated in planar GaAs MCs with the LP band of depth ~3 meV under optical pumping with ns-long pulses at a large angle with energy slightly above E_X. At variance with the conclusion drawn in Ref. 13, a strong depolarization of the photoexcited LPs was observed in the range of inflection points of the LP dispersion curve at both σ and π-polarized excitations. The prevailed direction of linear polarization of LPs in this range was found to coincide with the direction of the LP $\mathbf{k}$ vector rather than with the direction of the linear polarization of exciting pulses. The observed linear polarization of LP emission in the range of $k \sim k_{\text{infl}}$ corresponds to the emission of LP system with a partially thermalized distribution of LPs between the TE and TM modes.

In contrast, the polarization of the condensed LP mode at $k = 0$ and high P is linked to that of exciting pulses. It coincides with the polarization of the circularly polarized exciting pulses whereas the excitation with linearly polarized pulses results in the 90° rotation of the direction of condensate polarization.

The tight connection of LP condensate polarization to that of excited pulses in spite of the fact that the LP system at $k > 1\mu\text{m}^{-1}$ is highly depolarized enables us to conclude that the population of the condensed mode is mainly contributed by stimulated parametric LP-LP scattering directly in the driven mode rather than by that of LPs after multiple phonon-assisted scattering events. As a consequence, the formation of the LP condensate in shallow LP bands excited at large k slightly above exciton energy is to be described

within the framework of the optical parametric oscillator (OPO) model[23] rather than explained by quasi-equilibrium Bose-Einstein condensation. This conclusion is confirmed by the observed instability of the condensate mode in the range of nearly constant excitation density. Such instability is more characteristic of a nonlinear LP-LP scattering rather than the quasi-equilibrium Bose-Einstein condensate.

ACKNOWLEDGMENTS

We thank N. A. Gippius, L. E. Golub, S. G. Tikhodeev, and V. B. Timofeev for valuable remarks and fruitful discussions, and M. S. Skolnick for rendered samples. This work was supported by the Russian Foundation for Basic Research and the Russian Academy of Sciences.

[1] M. S. Skolnick, T. A. Fisher, and D. M. Whittaker, Semicond. Sci. Technol. **13**, 645 (1998).

[2] A. Kavokin and G. Malpuech, *Cavity Polaritons* (Elsevier, Amsterdam, 2003).

[3] H. Deng, G. Weihs, C. Santori, J. Bloch, and Y. Yamamoto, Science **298**, 199 (2002).

[4] M. Richard, J. Kasprzak, R. André, R. Romestain, Le Si Dang, G. Malpuech, and A. Kavokin, Phys. Rev. B **72**, 201301(R) (2005).

[5] J. Kasprzak, M. Richard, S. Kundermann, A. Baas, P. Jeambrun, J. M. J. Keeling, F. M. Marchetti, M. H. Szymanska, R. André, J. L. Staehli, V. Savona, P. B. Littlewood, B. Deveaud, and Le Si Dang, Nature (London) **443**, 409 (2006).

[6] R. Balili, V. Hartwell, D. Snoke, L. Pfeiffer, and K. West, Science **316**, 1007 (2007).

[7] J. J. Baumberg, A. V. Kavokin, S. Christopoulos, A. J. D. Grundy, R. Butté, G. Christmann, D. D. Solnyshkov, G. Malpuech, G. Baldassarri Hoger von Hogersthal, E. Feltin, J.-F. Carlin, and N. Grandjean, Phys. Rev. Lett. **101**, 136409 (2008).

[8] L. Klopotowski, A. Amo, M. D. Martin, L. Vina, I. A. Shelykh, M. M. Glazov, A. V. Kavokin, D. D. Solnyshkov, G. Malpuech, and R. André, Solid State Commun. **139**, 51 (2006).

[9] D. N. Krizhanovskii, K. G. Lagoudakis, M. Wouters, B. Pietka, R. A. Bradley, K. Guda, D. M. Whittaker, M. S. Skolnick, B. Deveaud-Plédran, M. Richard, R. André, and Le Si Dang, Phys. Rev. B **80**, 045317 (2009).

[10] M. D. Martin, G. Aichmayr, A. Amo, D. Ballarini, L. Klopotowski, and L. Vina, J. Phys. Condens. Matter **19**, 295204 (2007).

[11] J. Kasprzak, R. André, Le Si Dang, I. A. Shelykh, A. V. Kavokin, Y. G. Rubo, K. V. Kavokin, and G. Malpuech, Phys. Rev. B **75**, 045326 (2007).

[12] E. del Valle, D. Sanvitto, A. Amo, F. P. Laussy, R. André, C. Tejedor, and L. Vina, Phys. Rev. Lett. **103**, 096404 (2009).

[13] G. Roumpos, Chih-Wei Lai, T. C. H. Liew, Yu. G. Rubo, A. V. Kavokin, and Y. Yamamoto, Phys. Rev. B **79**, 195310 (2009).

[14] J. M. Kosterlitz and D. J. Thouless, J. Phys. C **6**, 1181 (1973).

[15] G. Cassabois, A. L. C. Triques, F. Bogani, C. Delalande, Ph. Roussignol, and C. Piermarocchi, Phys. Rev. B **61**, 1696 (2000).

[16] F. Tassone and Y. Yamamoto, Phys. Rev. B **59**, 10830 (1999).

[17] R. Butté, M. S. Skolnick, D. M. Whittaker, D. Bajoni, and J. S. Roberts, Phys. Rev. B **68**, 115325 (2003).

[18] P. G. Savvidis, J. J. Baumberg, R. M. Stevenson, M. S. Skolnick, D. M. Whittaker, and J. S. Roberts, Phys. Rev. Lett. **84**, 1547 (2000).

[19] A. I. Tartakovskii, D. N. Krizhanovskii, and V. D. Kulakovskii, Phys. Rev. B **62**, R13298 (2000).

[20] R. M. Stevenson, V. N. Astratov, M. S. Skolnick, D. M. Whittaker, M. Emam Ismail, A. I. Tartakovskii, P. G. Savvidis, J. J. Baumberg, and J. S. Roberts, Phys. Rev. Lett. **85**, 3680 (2000).

[21] V. D. Kulakovskii, A. I. Tartakovskii, D. N. Krizhanovskii, N. A. Gippius, M. S. Skolnick, and J. S. Roberts, Nanotechnology **12**, 475 (2001).

[22] N. A. Gippius, S. G. Tikhodeev, V. D. Kulakovskii, D. N. Krizhanovskii, and A. I. Tartakovskii, Europhys. Lett. **67**, 997 (2004).

[23] A. A. Demenev, A. A. Shchekin, A. V. Larionov, S. S. Gavrilov, V. D. Kulakovskii, N. A. Gippius, and S. G. Tikhodeev, Phys. Rev. Lett. **101**, 136401 (2008).

[24] J. Kasprzak, D. D. Solnyshkov, R. André, Le Si Dang, and G. Malpuech, Phys. Rev. Lett. **101**, 146404 (2008).

[25] H. Deng, D. Press, S. Götzinger, G. S. Solomon, R. Hey, K. H. Ploog, and Y. Yamamoto, Phys. Rev. Lett. **97**, 146402 (2006).

[26] H. Deng, H. Haug, and Y. Yamamoto, Rev. Mod. Phys. **82**, 1489 (2010).

[27] J. Levrat, R. Butte, E. Feltin, J.-F. Carlin, N. Grandjean, D. Solnyshkov, and G. Malpuech, Phys. Rev. B **81**, 125305 (2010).

[28] K. V. Kavokin, I. A. Shelykh, A. V. Kavokin, G. Malpuech, and P. Bigenwald, Phys. Rev. Lett. **92**, 017401 (2004).

[29] I. A. Shelykh, A. V. Kavokin, and G. Malpuech, Phys. Status Solidi B **242**, 2271 (2005).

[30] H. T. Cao, T. D. Doan, D. B. Tran Thoai, and H. Haug, Phys. Rev. B **77**, 075320 (2008).

[31] D. D. Solnyshkov, I. A. Shelykh, M. M. Glazov, G. Malpuech, T. Amand, P. Renucci, X. Marie, and A. V. Kavokin, Semiconductors **41**, 1080 (2007).

[32] T. Ostatnicky, D. Read, and A. V. Kavokin, Phys. Rev. B **80**, 115328 (2009).

[33] A. A. Demenev, A. A. Shchekin, A. V. Larionov, S. S. Gavrilov, and V. D. Kulakovskii, Phys. Rev. B **79**, 165308 (2009).

[34] D. M. Whittaker, Phys. Rev. B **63**, 193305 (2001).

[35] D. M. Whittaker, Phys. Rev. B **71**, 115301 (2005).

[36] M. Wouters and I. Carusotto, Phys. Rev. B **75**, 075332 (2007).

[37] C. Ciuti, P. Schwendimann, and A. Quattropani, Semicond. Sci. Technol. **18**, 279 (2003).

[38] V. E. Hartwell and D. W. Snoke, Phys. Rev. B **82**, 075307 (2010).

[39] S. Schumacher, N. H. Kwong, and R. Binder, Phys. Rev. B **76**, 245324 (2007).

[40] D. N. Krizhanovskii, D. Sanvitto, I. A. Shelykh, M. M. Glazov, G. Malpuech, D. D. Solnyshkov, A. Kavokin, S. Ceccarelli, M. S. Skolnick, and J. S. Roberts, Phys. Rev. B **73**, 073303 (2006).

[41] K. V. Kavokin, P. Renucci, T. Amand, X. Marie, P. Senellard, J. Bloch, and B. Sermage, Phys. Status Solidi C **2**, 763 (2005).

[42] H. T. Cao, T. D. Doan, D. B. Tran Thoai, and H. Haug, Phys. Rev. B **69**, 245325 (2004).

[43] J. Bloch and J. Y. Marzin, Phys. Rev. B **56**, 2103 (1997).

[44]F. P. Laussy, I. A. Shelykh, G. Malpuech, and A. Kavokin, Phys. Rev. B **73**, 035315 (2006).

[45]C. Ciuti, P. Schwendimann, and A. Quattropani, Phys. Rev. B **63**, 041303(R) (2001).

[46]S. S. Gavrilov, N. A. Gippius, S. G. Tikhodeev, and V. D. Kulakovskii, JETP **110**, 825 (2010).

[47]S. G. Tikhodeev, A. L. Yablonskii, E. A. Muljarov, N. A. Gippius, and Teruya Ishihara, Phys. Rev. B **66**, 045102 (2002).